The EMBO Journal (2010) 29, 1458–1471 | © 2010 European Molecular Biology Organization | All Rights Reserved 0261-4189/10
www.embojournal.org

THE EMBO JOURNAL

IBRDC2, an IBR-type E3 ubiquitin ligase, is a regulatory factor for Bax and apoptosis activation

Giovanni Benard[1], Albert Neutzner[2,4], Guihong Peng[1], Chunxin Wang[2], Ferenc Livak[3], Richard J Youle[2] and Mariusz Karbowski[1,*]

[1]Center for Biomedical Engineering and Technology, University of Maryland, Baltimore, MD, USA, [2]Biochemistry Section, National Institute for Neurological Disorders and Stroke, National Institutes of Health, Bethesda, MD, USA and [3]Department of Microbiology and Immunology School of Medicine, University of Maryland, Baltimore, MD, USA

Bax, a pro-apoptotic protein from the Bcl-2 family, is central to apoptosis regulation. To suppress spontaneous apoptosis, Bax must be under stringent control that may include regulation of Bax conformation and expression levels. We report that IBRDC2, an IBR-type RING-finger E3 ubiquitin ligase, regulates the levels of Bax and protects cells from unprompted Bax activation and cell death. Downregulation of IBRDC2 induces increased cellular levels and accumulation of the active form of Bax. The ubiquitination-dependent regulation of Bax stability is suppressed by IBRDC2 downregulation and stimulated by IBRDC2 overexpression in both healthy and apoptotic cells. Although mostly cytosolic in healthy cells, upon induction of apoptosis, IBRDC2 accumulates in mitochondrial domains enriched with Bax. Mitochondrial accumulation of IBRDC2 occurs in parallel with Bax activation and also depends on the expression levels of Bcl-xL. Furthermore, IBRDC2 physically interacts with activated Bax. By applying Bax mutants in HCT116 Bax$^{-/-}$ cells, combined with the use of active Bax-specific antibodies, we have established that both mitochondrial localization and apoptotic activation of Bax are required for IBRDC2 translocation to the mitochondria.

The EMBO Journal (2010) **29,** 1458–1471. doi:10.1038/emboj.2010.39; Published online 18 March 2010
Subject Categories: proteins; differentiation & death
Keywords: apoptosis; Bcl-2 family; protein degradation; ubiquitin ligase

Introduction

Apoptosis, a genetically driven form of cell death, results in a highly organized dismantling of dying cells. Decomposition of apoptotic cells is mediated by a family of proteases called caspases that in some modes of apoptosis are regulated by anti- and pro-apoptotic proteins from the Bcl-2 family. The main structural target of the Bcl-2 family in mammalian cells is the outer mitochondrial membrane (OMM). Bcl-2 proteins can either induce OMM permeabilization and thus apoptosis (e.g. Bax, Bak and Bok) or inhibit it and promote cell survival (e.g. Bcl-2, Bcl-xL and Mcl-1) (for reviews see Chipuk and Green, 2008; Youle and Strasser, 2008). Consequently, the ratio of pro-apoptotic versus anti-apoptotic Bcl-2 family members is a critical factor in regulating susceptibility to cell death (Wei *et al*, 2001). Various regulatory mechanisms, including regulation of Bcl-2 family protein expression, as well as diverse posttranslational modifications, regulate the balance of the activities of pro- and anti-apoptotic Bcl-2 family proteins in healthy cells, and upon induction of apoptosis. Accordingly, stress-induced expression of pro-apoptotic proteins, including Noxa or PUMA (Nakano and Vousden, 2001; Villunger *et al*, 2003), or changes in the phosphorylation status of pro-apoptotic Bad (Datta *et al*, 2002) can shift the Bcl-2 family balance toward apoptosis and cell death (for reviews see Adams and Cory, 2007; Youle and Strasser, 2008).

Recently, ubiquitin (Ub) conjugation and proteasomal degradation (UPS) (Hershko and Ciechanover, 1998) have also been shown to have a role in regulating apoptosis to some extent through direct effects on Bcl-2 family proteins. The degradation of anti-apoptotic factors, such as Bcl-2 and Mcl-1, is mediated by their polyubiquitination and requires the activity of the 26S proteasome (Breitschopf *et al*, 2000; Zhong *et al*, 2005; Azad *et al*, 2006). The 482-kDa HECT-domain-containing Ub ligase ARF-BP1/Mule (Mcl-1 Ub ligase E3) is necessary and sufficient for the regulation of Mcl-1 stability in DNA-damage-induced apoptosis (Zhong *et al*, 2005). Disappearance of Mcl-1, achieved by combined blockage of synthesis and degradation, is associated with the onset of apoptosis, indicating that regulation of the Mcl-1 protein level is essential for apoptosis induction (Cuconati *et al*, 2003; Zhong *et al*, 2005).

The apoptotic activities of Bid and Bax, the pro-apoptotic Bcl-2 family proteins, also seem to depend on the UPS system (Tait *et al*, 2007). Bax is a short-lived protein in malignant B-cell lines, and ubiquitination of Bax promotes its degradation in these cells (Agrawal *et al*, 2008). Supporting the importance of stringent regulation of Bax turnover, increased proteasomal degradation of Bax is a common feature of poor prognosis chronic lymphocytic leukaemia (Agrawal *et al*, 2008). The abnormal proteasome-dependent degradation of Bax also seems to be an important factor in the high resistance of malignant B cells to TRAIL-induced apoptosis. In these cells, TRAIL induces proteasome inhibition-sensitive, aberrant Bax degradation and makes these cells more resistant to apoptosis (Liu *et al*, 2008). It has also been shown that the turnover of the 24-kD splice variant of Bax (Baxβ) is higher than the turnover rate of the more abundantly expressed 21-kD Baxα (Fu *et al*, 2009). Given that Baxβ has a

*Corresponding author. Center for Biomedical Engineering and Technology, University of Maryland, Baltimore, 725 W. Lombard St, Baltimore, MD 21201, USA. Tel.: +410 706 4018; Fax: +410 706 8184; E-mail: karbowsk@umbi.umd.edu
[4]Present address: University Clinic Basel, Department for Biomedicine, Hebelstrasse 20, Basel 4031, Switzerland

Received: 2 October 2009; accepted: 18 February 2010; published online: 18 March 2010

stronger pro-apoptotic activity than Baxα (Fu *et al*, 2009), it has been proposed that proteasome-dependent degradation of this proteins is critical for cell survival (Fu *et al*, 2009). However, the mechanisms and molecular components that are vital for both Baxα and Baxβ ubiquitination and/or regulation of proteasomal degradation of these proteins remain unknown.

Our initial studies revealed that IBRDC2, an IBR-type RING-finger E3 Ub ligase that has already been implicated in p53-dependent apoptosis (Ng *et al*, 2003; Huang *et al*, 2006), accumulates on the mitochondria specifically upon apoptosis induction, in synchrony with Bax activation. Mitochondrial accumulation of IBRDC2 requires both Bax and apoptosis induction and does not occur in apoptotic $Bax^{-/-}$ cells. Although the ectopic expression of IBRDC2 increases Bax ubiquitination, downregulation of this protein leads to accumulation of an activated form of Bax and results in spontaneous apoptosis.

Results

IBRDC2 is a cytosol and mitochondria-localized RING-finger E3 Ub ligase

IBRDC2 (IBR domain containing 2), also known as p53-inducible RING-finger protein (p53RFP) or RNF144B (Ng *et al*, 2003; Huang *et al*, 2006), contains an in-between-ring (IBR)-type RING-finger domain (Marin *et al*, 2004) near its N-terminus (Figure 1A and B), predicted C-terminal transmembrane domain (Figure 1B). IBRDC2 is well conserved in higher eukaryotes, with orthologues in mouse (88% amino acid similarity), dog (95% amino acid similarity) and chicken (79% amino acid similarity). Yet, as in the case of other mitochondria-associated RING E3 ligases, including MARCH5/MARCH-V/MITOL (Nakamura *et al*, 2006; Yonashiro *et al*, 2006; Karbowski *et al*, 2007) and MULAN/MAPL/GIDE (Li *et al*, 2008; Zhang *et al*, 2008; Braschi *et al*, 2009), the database searches failed to detect any obvious orthologues of IBRDC2 in *S. cerevisiae* or *C. elegans* (data not shown). Western blot analyses of human tissue extracts showed that IBRDC2 is expressed in various tissues, with the highest levels detectable in heart, ovary, testis and spleen (Figure 1C).

In a majority of cells, yellow fluorescent protein-tagged IBRDC2 (YFP-IBRDC2) localized mainly to the cytosol, with a small subset of the protein showing a diffuse or vesicle-like distribution, partially associated with mitochondria (Figure 1D). However, in a small number of cells (~1%) YFP-IBRDC2 was highly enriched on the mitochondria (Figure 1E), as revealed by colocalization with Tom20, a marker of the OMM. This localization pattern was also detected using MYC-tagged IBRDC2 (MYC-IBRDC2) and C-terminal YFP fusion of IBRDC2 (IBRDC2-YFP), indicating that YFP fusion does not affect localization of IBRDC2 (Supplementary Figures S1 and S2). Similar localizations of YFP-IBRDC2 and MYC-IBRDC2 were detected in cells with diverse expression levels of these proteins, suggesting that

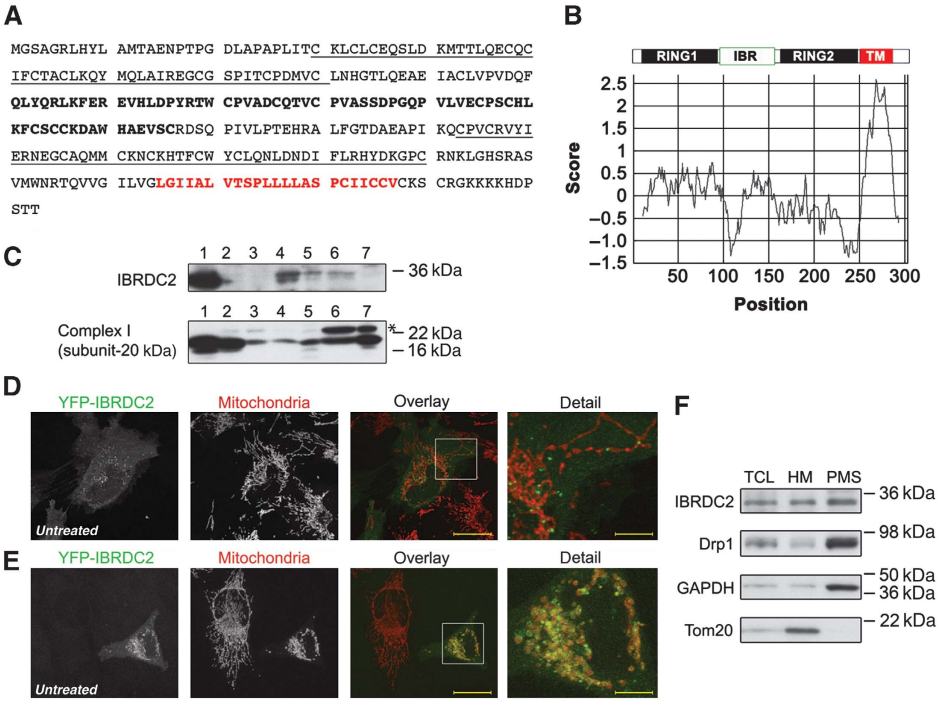

Figure 1 Identification of IBRDC2, a novel mitochondria-associated RING-finger protein. (**A**) Protein sequence of IBRDC2. IBRDC2 is an IBR-type RING-finger protein with predicted C-terminal transmembrane domain (red), and two RING-finger domains (underlined text) flanking in-between-ring domain (bold). (**B**) Schematic representation of IBRDC2 domains and Kyte–Doolittle plot revealing a predicted transmembrane domain. (**C**) The expression patterns of IBRDC2 in various human tissues. A total of 25 μg of human tissue lysates (Imgenex) was resolved by SDS–PAGE and analysed for IBRDC2 with anti-IBRDC2 mAb; anti-mitochondrial respiratory complex I (subunit 20 kD) mAb was used as control. The tested tissue samples were: (1) heart, (2) kidney, (3) liver, (4) ovary, (5) testis, (6) spleen and (7) brain. (**D**, **E**) HeLa cells transfected with YFP-IBRDC2 (green) were immunostained with anti-cytochrome *c* mAb (red) and analysed by confocal microscopy. Right panels show detailed images of the areas marked with white rectangles. Bars: 20 μm (overlay), 5.5 μm (detail). (**F**) A total of 40 μg of total cell lysates (TCLs), mitochondria-enriched heavy membrane (HM) pellets and post mitochondrial supernatants (PMS) were analysed by western blot using antibodies indicated in the figure.

the variability in subcellular localization of IBRDC2 is not due to ectopic expression. As the anti-IBRDC2 antibodies were not applicable for immunofluorescence, we applied subcellular fractionation followed by western blot analysis of endogenous IBRDC2. This assay showed a high degree of IBRDC2 association with the mitochondria-enriched heavy membrane fraction (HM), yet a significant part of this protein was also detected in the postmitochondrial supernatant fraction (PMS; Figure 1F).

We noted that in cells with mitochondria-accumulated YFP-IBRDC2, mitochondrial fragmentation was readily apparent (Figure 1E; detail). As mitochondrial fragmentation is often associated with functional changes in these organelles, these data suggest that, as in the case of Parkin (Narendra *et al*, 2008) and SenP5 (Zunino *et al*, 2007), the proteins implicated in ubiquitination or SUMOylation of mitochondrial proteins, mitochondrial accumulation of IBRDC2 might be regulated by the functional state of mitochondria or a mitochondria-related signal.

Induction of apoptosis triggers mitochondrial accumulation of IBRDC2

To test this possibility, YFP-IBRDC2-overexpressing cells were treated with (1) m-chlorocarbonyl cyanide phenylhydrazone (CCCP), a mitochondrial uncoupler and inducer of permeability transition (PT) and (2) inducers of mitochondria-dependent apoptosis: actinomycin D (ActD), a DNA replication and transcription inhibitor; staurosporine (STS), a general kinase inhibitor; and tunicamycin (Tun), an inhibitor of protein glycosylation in the ER. In addition, mitochondrial function was perturbed using local laser irradiation of TMRE-labelled mitochondria in living cells, as described by De Giorgi *et al* (2002). This induces mitochondrial permeability transition and subsequent mitochondrial damage (De Giorgi *et al*, 2002). To avoid caspase activation-induced detachment of apoptotic cells, cells were pretreated with a caspase inhibitor zVAD-fmk before respective treatments. Cells were fixed, immunostained for Tom20 and analysed using fluorescence microscopy. The data showed an extensive redistribution of IBRDC2 from the cytosol to the mitochondria in cells treated with ActD (Figure 2A and C), STS (Figure 2B and C) and Tun (Figure 2C), but not in CCCP-treated cells (Figure 2C), or cells with photodamaged mitochondria. Furthermore, in cells co-transfected with IBRDC2 and Bcl-xL, an anti-apoptotic protein from the Bcl-2 family, ActD and STS failed to induce mitochondrial translocation of IBRDC2 (Figure 2C), indicating that apoptosis induction is a prerequisite for this process. The extent of colocalization of IBRDC2 with Tom20 (mitochondria), GM130 (Golgi complex) and LAMP1 (lysosomes) was analysed using quantification of pixel distribution in red (mitochondria, Golgi complex or lysosomes) and green (IBRDC2) channels of images using the colocalization module of the AxioVision4 software (Zeiss). As revealed by Pearson's correlation values, in ActD- and STS-treated cells with punctiform IBRDC2 distribution, colocalization of IBRDC2 with mitochondria, but not with the Golgi complex or lysosomes, was detected (Figure 2D). There was no colocalization between the analysed organelles and IBRDC2 in healthy cells (Figure 2D). Thus, the majority of IBRDC2 relocates from the cytosol to the mitochondria, but not to other tested organelles, specifically in apoptotic cells. Next, cells treated with ActD and STS and also DMSO-treated control cells were fractionated into mitochondria-enriched HM fractions and PMS cytosolic fractions followed by western blot. Consistent with the immunofluorescence results, a substantial redistribution of endogenous IBRDC2 from the PMS to the mitochondria-enriched HM fractions was detected in both ActD- and STS-treated cells (Figure 2E).

Mitochondrial accumulation of IBRDC2 correlates with cytochrome c release, depends on a predicted transmembrane domain and is modulated by RING domain activity

Cytochrome *c* is a mitochondrial intermembrane space protein released from the mitochondria to the cytosol early during apoptosis (Kluck *et al*, 1997). To test the temporal relation of mitochondrial accumulation of IBRDC2 and OMM permeabilization, cells expressing YFP-IBRDC2 were treated with ActD or STS, immunostained for cytochrome *c* and then analysed by microscopy (Figure 3). In ActD- or STS-treated cells with mitochondria-accumulated YFP-IBRDC2, cytochrome *c* was released into the cytosol (Figure 3A and D), indicating a high correlation between the OMM permeabilization and mitochondria accumulation of YFP-IBRDC2.

To test the mechanism of mitochondrial translocation of IBRDC2, we constructed: (1) an IBRDC2 mutant lacking a predicted transmembrane domain (amino acid residues 1–258; IBRDC2Δ^{TM}), (2) a fragment that includes the predicted transmembrane domain but not the C-terminal part of the protein (amino acid residues 258–303; IBRDC2^{TM}) and (3) a mutant expected to inhibit the zinc coordination in the two RING domains of IBRDC2, and thus the E3 Ub ligase activity of this protein (H161W, H216W; IBRDC2^{RING-}). The subcellular localization of these proteins was analysed in healthy and apoptotic cells (Figure 3). The data showed that YFP-IBRDC2Δ^{TM} localized to the cytosol in healthy cells and, unlike YFP-IBRDC2, failed to translocate to the mitochondria upon induction of apoptosis (Figure 3B and D). YFP-IBRDC2 showed a diffuse localization in healthy cells (Supplementary Figure S3) but localized to mitochondria in apoptotic cells (Figure 3C and D; Supplementary Figure S3). Thus, the predicted transmembrane domain of IBRDC2 is essential for the IBRDC2 response to apoptotic triggers. As YFP-IBRDC2^{RING-} also localized to the cytosol in healthy cells (data not shown), but mitochondrial association of YFP-IBRDC2^{RING-} was noticeable only in $\sim$50% of apoptotic cells (Figure 3D), one can conclude that the activity of the RING domain also contributes to changes in the cellular distribution of IBRDC2.

IBRDC2 regulates cellular levels of Bax

To date, a majority of RING domain proteins, including IBR proteins, are thought to possess E3 Ub ligase activity (Joazeiro and Weissman, 2000; Fang *et al*, 2003; Marin *et al*, 2004). The most common outcome of protein ubiquitination is a subsequent proteasomal degradation of target proteins (Hershko and Ciechanover, 1992). The reported E3 Ub ligase properties of IBRDC2 (Ng *et al*, 2003; Huang *et al*, 2006) prompted us to test whether downregulation of IBRDC2 affects proteins associated with mitochondrial steps in apoptosis. We applied short hairpin RNA interference (shRNAi) to downregulate IBRDC2 expression; a construct targeting green fluorescent protein was used as a control (Control RNAi).

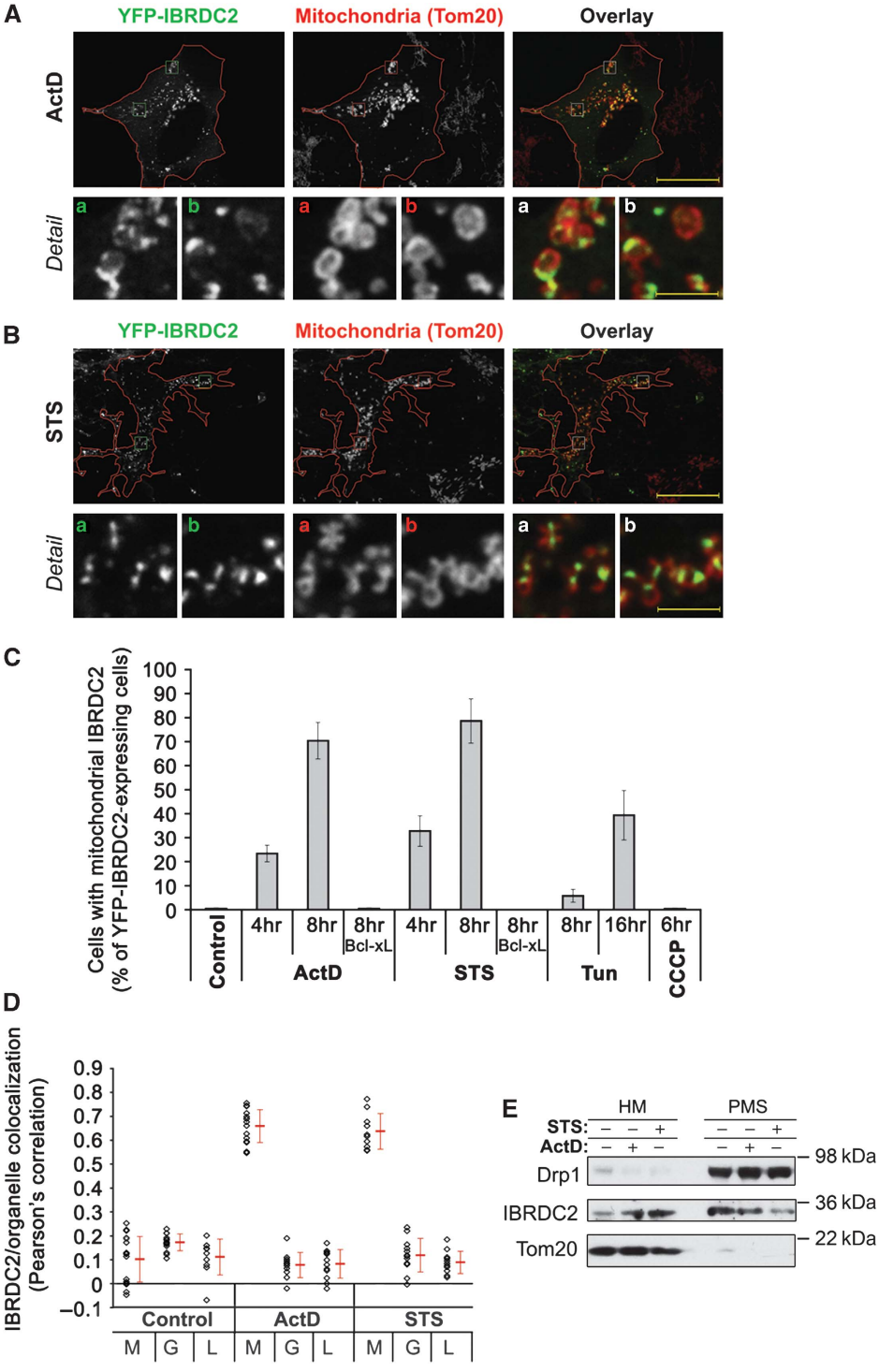

Figure 2 Apoptosis-induced mitochondrial accumulation of IBRDC2. (**A**, **B**) HeLa cells were transfected with YFP-IBRDC2 (green). At 18 h after transfection, cells were treated with 10 μM ActD (**A**) or 1 μM STS (**B**). To prevent detachment of apoptotic cells, 50 μM zVAD-fmk was added ~30 min before addition of ActD and STS. Cells were immunostained with anti-Tom20 mAb (red), followed by fluorescent microscopy analysis. Bars: 20 μm (overlay), 2.3 μm (detail). (**C**) Quantification of the number of cells expressing YFP-IBRDC2 showing mitochondrial accumulation of IBRDC2 after treatments with ActD, STS, Tun, and CCCP, as specified in the figure. Cells were also co-transfected with YFP-IBRDC2 and CFP-Bcl-xL and mitochondrial translocation of IBRDC2 was quantified in ActD- and STS-treated YFP-IBRDC2 and CFP-Bcl-xL expressing cells. Data represent the average ± s.d. of three experiments with >200 cells/condition counted each time. (**D**) Colocalization of IBRDC2 with mitochondria (M), Golgi complex (G) and lysosomes (L) was analysed in untreated cells and cells treated with ActD or STS. The values represent Pearson's correlation units (*r*) that reveal the degree of association of pixels in different channels of the image. Data represent the average ± s.d. of >15 cells/condition. Values obtained from each measurement are also shown (black diamonds). (**E**) Control HeLa cells, or cells treated with ActD or STS, were fractionated into heavy membrane (HM) and cytosolic fractions (PMS) followed by western blot analysis for the subcellular distribution of endogenous IBRDC2.

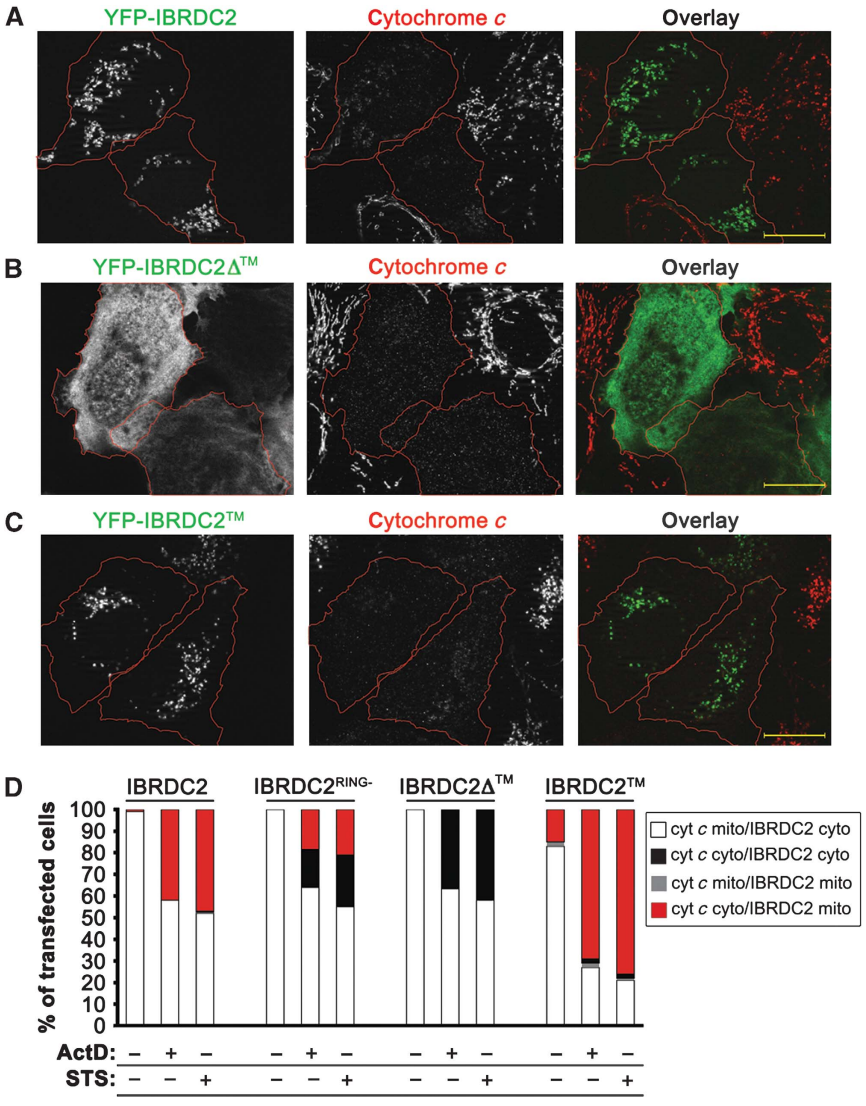

Figure 3 Mechanism of mitochondrial translocation of IBRDC2. (**A–C**) Cells transfected with YFP-IBRDC2 (**A**), YFP-IBRDC2Δ^{TM} (**B**) and YFP-IBRDC2^{TM} (**C**) (green) were treated with ActD, and then immunostained with anti-cytochrome *c* mAb (red). Bars: 20 μm. (**D**) Quantification of the number of cells expressing (1) YFP-IBRDC2, (2) YFP-IBRDC2 RING domain mutant (YFP-IBRDC2^{RING-}), (3) YFP-IBRDC2, (4) YFP-IBRDC2Δ and (5) YFP-IBRDC2^{TM} showing mitochondrial accumulation of IBRDC2, versus subcellular localization of cytochrome *c* after treatments with ActD or STS. A typical experiment with >300 cells/condition is shown.

Total cell lysates of IBRDC2 RNAi and Control RNAi cells were resolved with SDS–PAGE followed by blotting with antibodies against various apoptosis-related proteins such as Bax, Bak, Mcl-1, Bcl-2 and Bcl-xL (Figure 4A and data not shown). Among the tested proteins, the protein level of Bax was substantially increased by IBRDC2 downregulation (Figure 4A). The quantification of Bax level changes in several independent experiments revealed that downregulation of IBRDC2 induces 1.93 ± 0.49-fold increase ($n = 5$) in Bax levels when compared with Control RNAi cells. As the levels of all analysed members of the Bcl-2 protein family, except Bax but including Bak, the closest Bax homologue (Wei *et al*, 2001), were not altered by IBRDC2 knockdown, this effect seems to be highly specific. This result was confirmed using two other effective IBRDC2 shRNAi constructs (Figure 4B). In addition, IBRDC2 downregulation in human colorectal cancer cells (HCT116) also induced Bax accumulation (Figure 4C). Thus, lowered IBRDC2 protein levels are primary factors leading to cellular accumulation of Bax, suggesting a role for IBRDC2 in the regulation of Bax stability. Furthermore, Bax level decreases were more pronounced in protein inhibitor, cycloheximide (CHX)-treated Control RNAi cells than in IBRDC2 RNAi cells (Supplementary Figure S4A), suggesting that IBRDC2 regulates stability of Bax.

Role of IBRDC2 in Ub-dependent regulation of Bax

To test the mechanism by which IBRDC2 regulates the steady-state levels of Bax, we first analysed the effects of the proteasome inhibitor MG132 on Bax turnover. As, in addition to proteasomal degradation, the relative rates of ubiquitination and deubiquitination can also regulate the fate and function of Ub-conjugated proteins (Figure 5A), we also tested the effect of a specific inhibitor of de-ubiquitinating enzymes (DUBs) on Bax levels. The activity of DUBs is sensitive to 4H-Thiopyran-4,one,tetrahydro-3,5-bis[(4-nitrophenylmethylene]-,1,1-dioxide (G5) (Aleo *et al*, 2006; Fontanini *et al*, 2009). The data showed that although an

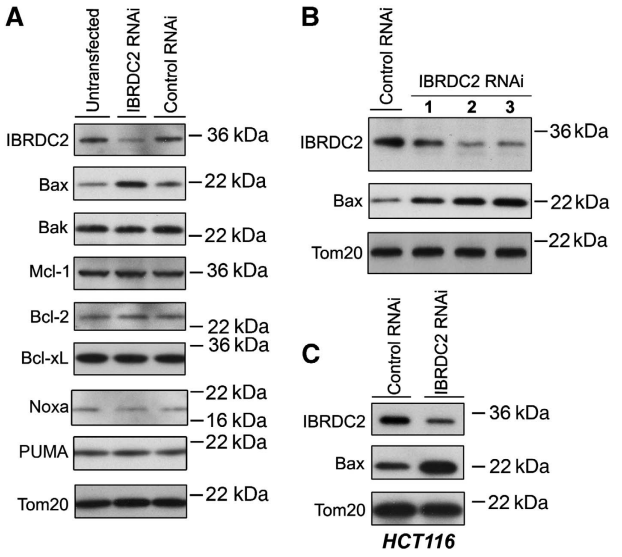

Figure 4 Downregulation of IBRDC2 induces an abnormal accumulation of Bax. The IBRDC2 expression in HeLa (**A**, **B**), and HCT116 (**C**) cells was downregulated using the shRNAi method. The total cell lysates were resolved with SDS–PAGE followed by immunoblotting for various apoptosis-related proteins as indicated in the figure. In **B** three different IBRDC2 shRNAi constructs were tested; no. 3 represents the construct used in **A**, **C** and all other experiments.

accumulation of the short-lived protein Mcl-1 was detected as early as 2 h after MG132 treatment (Figure 5B), no increase in either 21-kD Baxα or the recently characterized 24-kD Baxβ (Fu *et al*, 2009) was detected even at 6 h of MG132 treatment (Figure 5B). Consistent with a recent study (Fu *et al*, 2009), 24-kD Baxβ was detected after a prolonged 15 h treatment with MG132, yet we did not detect any noticeable changes in the level of Baxα (Supplementary Figure S4B and C). Thus, when compared with Mcl-1, the steady-state stability of both Bax variants, and of Baxα in particular, is high. Cells treated with G5 for 2 h, 4 h and 6 h were analysed using western blot (Figure 5B). As expected, treatment with G5 resulted in an increase in the pool of ubiquitinated proteins and a decrease in a monomeric Ub (Figure 5B). Notably, G5 treatment also induced a gradual decrease in Bax levels, suggesting that inhibition of Bax deubiquitination leads to the destabilization of this protein.

We also tested whether G5 stabilizes the ubiquitinated form of Bax. To achieve this, HA-tagged Ub (HA-Ub) was immunoprecipitated from cells treated with G5, and tested by western blot for Bax. The data showed that Bax coimmunoprecipitated with HA-Ub in a G5-dependent manner (Figure 5C).

If IBRDC2 is required for Bax ubiquitination, then downregulation of IBRDC2 should decrease the effects of G5 on steady-state levels of Bax, whereas overexpression of IBRDC2 would augment these effects (Figure 5D). To test this hypothesis, we first examined whether downregulation of IBRDC2 influences G5-induced changes in the Bax levels in healthy cells and upon induction of apoptosis. IBRDC2 RNAi and Control RNAi cells were treated with G5 for 2 h, with STS for 6 h or left untreated. In one group of STS-treated cells, G5 was added after 4 h into STS treatment. Total cell lysates were analysed using western blot (Figure 5D). The data showed that although a decrease in Bax levels was induced by G5 treatment in both healthy and STS-treated Control RNAi cells, the levels of Bax were slightly increased by G5 treatment in IBRDC2 RNAi cells. Overall accumulation of ubiquitinated proteins was not changed in IBRDC2 RNAi cells (Figure 5D). We also analysed the role of IBRDC2 in the regulation of Bax stability using cells transfected with MYC-tagged wild-type (WT) IBRDC2 (MYC-IBRDC2) or mutated IBRDC2 (MYC-IBRDC2Δ^{TM}), with pEYFP vector as a control (Figure 5E). Cells were treated with G5 for 2 h or 6 h, with STS for 6 h or left untreated. In one group of STS-treated cells, G5 was added at 4 h into treatment as before. The data showed that G5-induced decreases in monomeric Bax were associated with a moderate increase in high-molecular-weight Bax in cells expressing MYC-IBRDC2^{TM} when compared with control cells (Figure 5E). STS-induced changes in Bax mobility were extensively stabilized by G5 in cells expressing MYC-IBRDC2, but not detectably so in control cells or cells expressing MYC-IBRDC2Δ, indicating that IBRDC2 participates in Bax ubiquitination. The lack of a major difference in the amount of the STS/G5-induced high-molecular-weight form of Bax between control cells and cells expressing MYC-IBRDC2Δ^{TM} (Figure 5E) indicates that mitochondrial translocation of IBRDC2 might be required for Bax ubiquitination detected in STS/G5-treated cells.

Synchronous mitochondrial translocation of IBRDC2 and Bax

Similar to IBRDC2, in healthy cells Bax resides in both the cytosol and on mitochondria (Hsu *et al*, 1997; Hsu and Youle, 1998), but it accumulates on mitochondria during the early stages of apoptosis (Hsu *et al*, 1997; Hsu and Youle, 1998). Moreover, Bax as well as Bak, the OMM-resident homologue of Bax, are required for, or participate in, OMM permeabilization, mitochondrial fragmentation and subsequent activation of caspases and mitochondrial damage (Wei *et al*, 2001; Karbowski *et al*, 2002; Schinzel *et al*, 2004). To test the time of IBRDC2 mitochondrial translocation in relation to changes in the subcellular localization of Bax, cells coexpressing YFP-IBRDC2 and CFP-tagged human Bax (CFP-Bax) were pre-incubated with zVAD-fmk, treated with STS and then analysed using time-lapse confocal microscopy. The data showed a highly synchronized mitochondrial accumulation of YFP-IBRDC2 and CFP-Bax (Figure 6A). The quantification of single-cell experiments (Figure 6B) showed a high statistical correlation of the mitochondrial accumulation times of IBRDC2 and Bax ($r_{IBRDC2/Bax} = 0.946 \pm 0.048$; $n = 10$, with the values between 0.7 and 1.0 being indicative of the strong positive correlation). Given that mitochondrial translocation of other pro-apoptotic members of the Bcl-2 family, including Bid and Bad, often does not correlate with mitochondrial accumulation of Bax (Nechushtan *et al*, 2001), these data further support a functional link between IBRDC2 and Bax.

Spatial relation of Bax and IBRDC2 on the mitochondria

Quantitative analyses of the colocalization between Tom20, a homogenously distributed marker of the OMM, and Bax, or between Tom20 and IBRDC2, revealed that in both ActD- and STS-treated apoptotic cells, ~90% of Bax or ~90% of IBRDC2 colocalized with ~50% of Tom20 (Figure 7A). These data support the observation that both Bax (Nechushtan *et al*, 2001; Karbowski *et al*, 2002) and

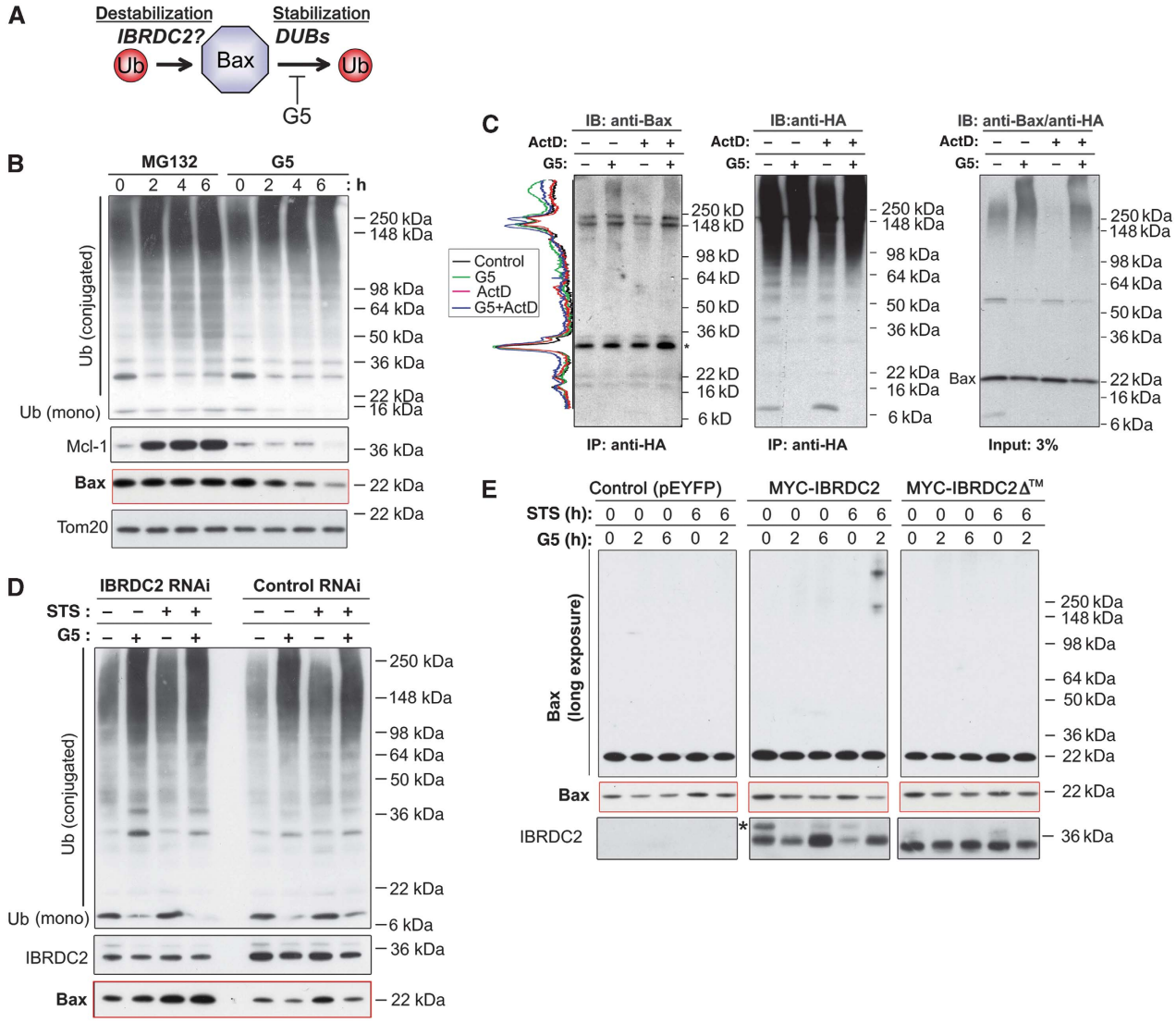

Figure 5 Role of IBRDC2 in ubiquitination-dependent regulation of Bax. (**A**) Schematic depiction of the potential role of IBRDC2-mediated ubiquitination and deubiquitination in the regulation of Bax stability. (**B**) HeLa cells were treated with proteasome inhibitor (MG132; 10 μM) or Ub isopeptidase inhibitor (G5; 5 μM) for 0 h, 2 h, 4 h and 6 h. The total cell lysates were resolved with SDS–PAGE followed by immunoblotting for proteins indicated in the figure. (**C**) The SDS/Triton X-100 cell lysates of HA-Ub-transfected HeLa cells that were treated with G5 in the presence or absence of ActD were immunoprecipitated with anti-HA mAb. The immunoprecipitating complexes were resolved with SDS–PAGE and analysed by western blot as indicated in the figure. Profile plots of Bax (left) were generated using ImageJ software. The protein amounts in each sample were normalized to the levels of light chain (indicated with *). Note an increase in high-molecular-weight species of Bax accumulating in the presence of G5. (**D**) IBRDC2 RNAi and Control RNAi cells were treated with G5 for 2 h, with STS for 6 h or left untreated. In one group of STS-treated cells, G5 was added at 4 h of treatment, followed by 2 h of additional incubation. Total cell lysates were resolved with SDS–PAGE followed by western blot as indicated in the figure. (**E**) HeLa cells transfected with MYC-tagged wild-type IBRDC2 (MYC-IBRDC2), MYC-IBRDC2Δ^{TM} and pEYFP vector as a control were treated with G5 for 2 h or 6 h, with STS for 6 h or left untreated. In one group of STS-treated cells, G5 was added at 4 h of treatment, followed by 2 h of additional incubation. Total cell lysates were resolved with SDS–PAGE followed by western blot as indicated in the figure. Note that MYC-IBRDC2 is an unstable protein and is destabilized by apoptosis-inducing triggers. *Top band likely represent posttranslational modification of MYC-IBRDC2 that can be also detected when endogenous protein is tested.

IBRDC2 (see Figure 2) localize in discrete submitochondrial domains, which in both cases cover ~50% of the OMM area. Furthermore, the detected overlap of ~80% of Bax and ~80% of IBRDC2 (Figure 7A) indicates that Bax and IBRDC2 probably localize to the same domains on mitochondria. Indeed, the high-resolution fluorescent images of apoptotic cells expressing YFP-IBRDC2 and immunostained for Bax and Tom20 (Figure 7B and C) revealed that Bax and IBRDC2 either colocalize or are adjacent to each other within the same submitochondrial structures in both ActD- (Figure 7B) and STS-treated cells (Figure 7C). Using Blue-Native gel electrophoresis (BN-PAGE) combined with SDS–PAGE of mitochondrial fractions isolated from ActD- and STS-treated cells, we also found that a subset of Bax is distributed in a similar manner to a subset of IBRDC2 (Supplementary Figure S5).

Bax and apoptotic triggers are required for the mitochondrial accumulation of IBRDC2

Taking into account that Bax and IBRDC2 cotranslocate to mitochondria and that these proteins colocalize in discrete submitochondrial domains, we tested whether apoptosis-

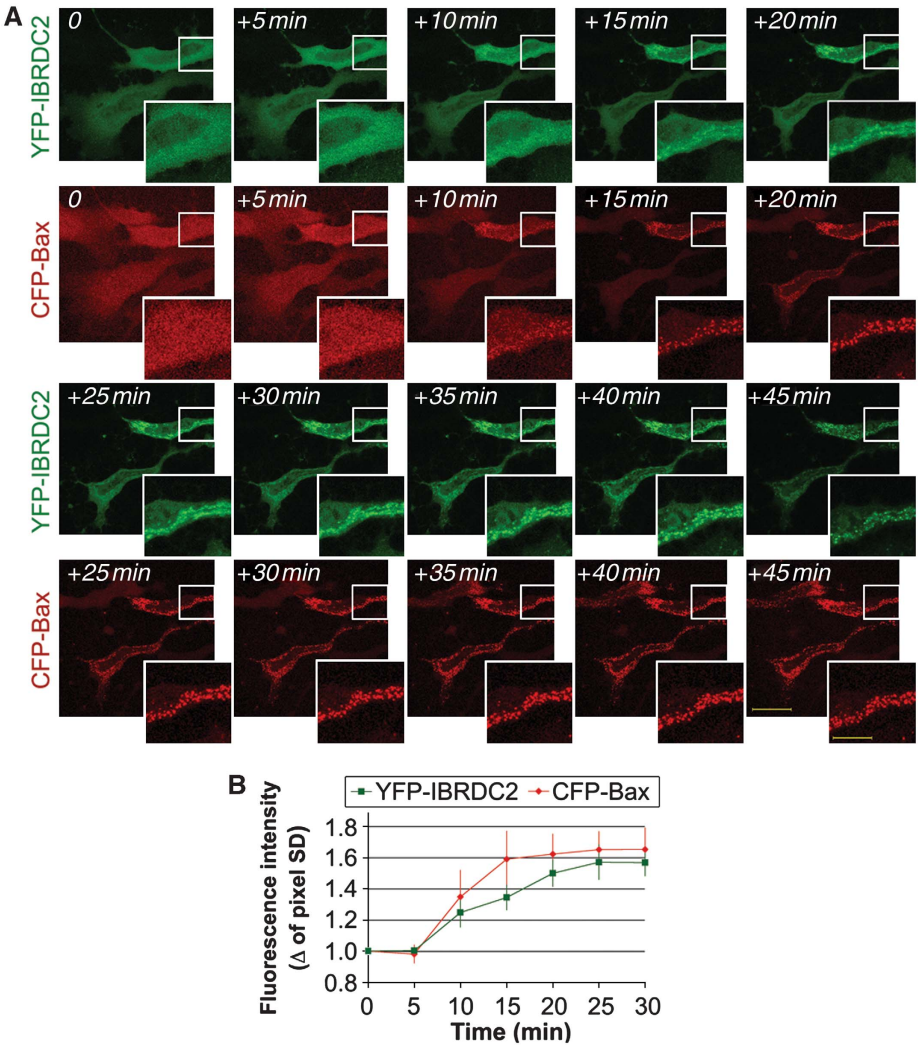

Figure 6 Synchronous mitochondrial translocation of IBRDC2 and Bax. HeLa cells were co-transfected with YFP-IBRDC2 (green) and CFP-Bax (red). Cells were pretreated with zVAD-fmk, to abolish detachment of apoptotic cells, followed by treatment with 1 μM STS. (**A**) An example of a time-lapse experiment. Bars: 20 μm, 10 μm (detail image). (**B**) The averaged pixel s.d. from 10 single-cell measurements obtained on two separate occasions, representing shifts from a more homogenous distribution to increased variability, were quantified using Metamorph image analysis software (Molecular Devices) and are plotted against the time of treatment. The traces shown in (**B**) were scaled so that the images obtained 10 min before detectable changes in pixel s.d. were used as 0 min.

induced mitochondrial accumulation of IBRDC2 requires Bax and/or whether mitochondrial accumulation of Bax depends on IBRDC2. HCT116 Bax$^{-/-}$ cells were transfected with YFP-IBRDC2 alone (Figure 8A) or together with CFP-Bax (Figure 8B) or CFP-Bak (Figure 8C), immunostained for cytochrome *c* and analysed using confocal microscopy. Given that Bax and Bak overexpression are strong pro-apoptotic signals leading to apoptotic cell death without additional external stimuli (Nechushtan *et al*, 1999; Schinzel *et al*, 2004), cells were fixed and analysed ~18 h after transfection without any further treatment. Apoptosis induction in both Bax- and Bak-overexpressing HCT116 Bax$^{-/-}$ cells was evidenced by cytochrome *c* release from the mitochondria to the cytosol (Kluck *et al*, 1997) (Figure 8A–D). YFP-IBRDC2-expressing HCT116 Bax$^{-/-}$ cells (Figure 8A) or HCT116 Bax$^{-/-}$ cells co-transfected with either YFP-IBRDC2 and CFP-Bax (Figure 8B) or YFP-IBRDC2 and CFP-Bak (Figure 8C) were grouped based on the subcellular localization of cytochrome *c* and IBRDC2 (Figure 8D). The data showed that although in ~100% of Bax-expressing HCT116 Bax$^{-/-}$ cells with cytosolic cytochrome *c*, YFP-IBRDC2 localized to mitochondria, the mitochondrial accumulation of YFP-IBRDC2 was not detected in apoptotic HCT116 Bax$^{-/-}$ cells overexpressing CFP-Bak (Figure 8D). In none of the control cells was cytochrome *c* release and mitochondrial localization of IBRDC2 detected (Figure 8A and D). Thus, considering that in HCT116 Bax$^{-/-}$ cells only Bax, but not Bak, overexpression-induced apoptosis triggers mitochondrial translocation of IBRDC2, one can conclude that Bax regulates the subcellular distribution of IBRDC2.

Next we asked whether mitochondrial localization of Bax is sufficient to induce mitochondrial translocation of IBRDC2 in non-apoptotic cells. HCT116 Bax$^{-/-}$ cells were transfected with YFP-IBRDC2 together with CFP-tagged Bax^{S184V} (CFP-Bax^{S184V}). Similar to WT Bax, ectopic expression of Bax^{S184V} is a potent pro-apoptotic trigger (Nechushtan *et al*, 1999); however, Bax^{S184V} also localizes exclusively to the mitochondria in non-apoptotic cells (Nechushtan *et al*, 1999). To reveal

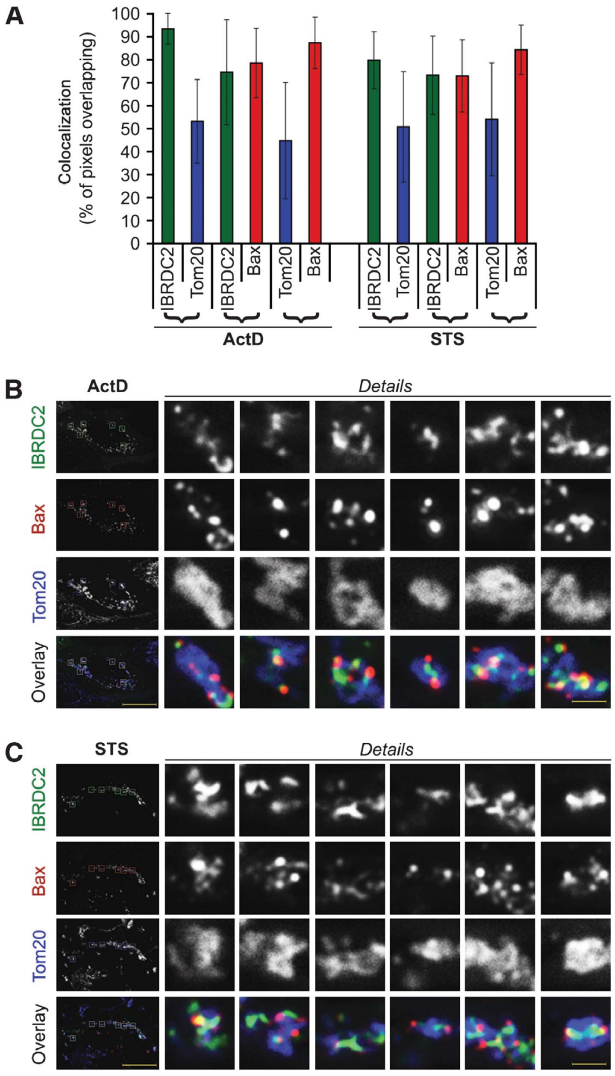

Figure 7 Submitochondrial localization of IBRDC2 and Bax. Cells transfected with YFP-IBRDC2 (green in **B**, **C**) were treated with ActD (**A**, **B**) and STS (**A**, **C**) followed by immunostaining for Tom20 (blue on overlay images in **B**, **C**) and Bax (red in **B**, **C**). Bars: 20 μm and 1.3 μm (detail images). (**A**) Images were analysed for pixel overlap between green (IBRDC2) and red (Bax), green and blue (Tom20) and red and blue channels using colocalization module of image acquisition and analysis software AxioVison 4 (Zeiss). Data represent the average ± s.d. ($n = 78$ images in ActD-treated cells and 66 images in STS-treated cells).

apoptotic activation of Bax, cells were immunostained with anti-Bax 6A7 antibody that binds to an epitope that is hidden in healthy cells and becomes antibody accessible upon induction of apoptosis (Hsu and Youle, 1998). The data showed that in non-apoptotic cells (Bax 6A7 epitope-negative) expressing CFP-Bax^{S184V}, YFP-IBRDC2 localized to the cytosol (Figure 8E and G). In contrast, apoptotic cells (Bax 6A7 epitope-positive) expressing CFP-Bax^{S184V} showed mitochondrial localization of YFP-IBRDC2 (Figure 8F and G). This indicates that the apoptosis-associated change(s) in Bax conformation is required for mitochondrial accumulation of IBRDC2. Furthermore, western blot analyses showed that Bax re-expression, but not ectopic expression of Bak, increases the amount of endogenous IBRDC2 associated with mitochondria in ActD-treated HCT116 Bax$^{-/-}$ cells (Figure 8H).

It has been shown that whereas Triton X-100 readily exposes the 6A7 Bax epitope, Chaps does not expose this epitope (Hsu and Youle, 1998). To determine whether IBRDC2 can physically interact with active Bax, we used the immunoprecipitation of Triton X-100 or Chaps cell lysates with anti-Bax 6A7 antibodies (Figure 8I). Furthermore, as viral mitochondria-associated inhibitor of apoptosis (vMIA) can bind and stabilize Bax in a non-apoptotic conformation (Arnoult *et al*, 2004; Norris and Youle, 2008), Bax 6A7 immunoprecipitations using vMIA-expressing cell lysates were used as control. The data showed that although IBRDC2 can be detected in samples obtained from Triton X-100 immunoprecipitates of control cells (Figure 8I), it is not detectable in Triton X-100 immunoprecipitates obtained from vMIA-transfected cells, even though similar amounts of Bax were detected (Figure 8I). Thus, one can conclude that coimmunoprecipitation of IBRDC2 with Bax 6A7 is specific, and regulated by Bax conformation controlling factors (e.g. vMIA). Supporting the specificity of the IBRDC2 interaction with Bax 6A7, we did not detect any Bax and IBRDC2 in Chaps lysates (Figure 8I).

In contrast to the critical role of 6A7 epitope-positive Bax in mitochondrial accumulation of IBRDC2, IBRDC2 is not required for mitochondrial translocation of Bax. Conversely, a significant increase in mitochondrial translocation of Bax ($7.94 \pm 1.58\%$ of cells; $n > 200$), when compared with Control RNAi cells ($0.3 \pm 0.26\%$ of cells; $n > 200$), was apparent. To reveal the functional status of Bax (6A7 positive versus 6A7 negative) in Control RNAi and IBRDC2 RNAi cells, we applied immunoprecipitation using anti-Bax 6A7 antibody. As revealed by Bax 6A7 immunoprecipitation from Chaps lysates obtained from Control RNAi and IBRDC2 RNAi cells, downregulation of IBRDC2 leads to a striking accumulation of 6A7 epitope-positive Bax in IBRDC2 RNAi cells when compared with Control RNAi cells (Figure 8J). Amounts of 6A7 epitope-positive Bax, only slightly higher than from Chaps lysates of IBRDC2 RNAi cells, were immunoprecipitated from Triton X-100 lysates of both Control RNAi and IBRDC2 RNAi cells. Thus, one can conclude that IBRDC2 downregulation leads to a very extensive increase in 6A7 epitope-positive Bax. Consistently, as revealed using BN-PAGE, the levels of oligomeric Bax were also largely increased in IBRDC2 RNAi cells, without apparent changes in monomeric Bax (Figure 8K), when compared with Control RNAi cells.

The role of IBRDC2 in the regulation of apoptosis

The apoptotic responses of IBRDC2 RNAi cells and Control RNAi cells upon treatment with ActD and STS were examined. To this end, apoptotic cleavage of the caspase substrate Poly (ADP-ribose) polymerase (PARP), as well as caspase-3 and -9 activation (Figure 9A), was assayed using western blotting. The data showed major increases in PARP cleavage (Figure 9A and B) as well as caspase-3 and -9 processing (Figure 9A) in both untreated and apoptosis-inducing agent-treated IBRDC2 RNAi cells when compared with Control RNAi cells. Furthermore, FACS analyses of cells incubated for 1 h with a fluorescent cell-permeable inhibitor of caspase-3 and -7 (FLICA) revealed a three- to four-fold increase in the number of FLICA-positive cells in IBRDC2 RNAi cells when compared with Control RNAi cells (20.6 ± 0.4 versus $5.7 \pm 0.1\%$ of cells, respectively, in the experiment shown in Figure 9C). The higher number of FLICA-positive cells in

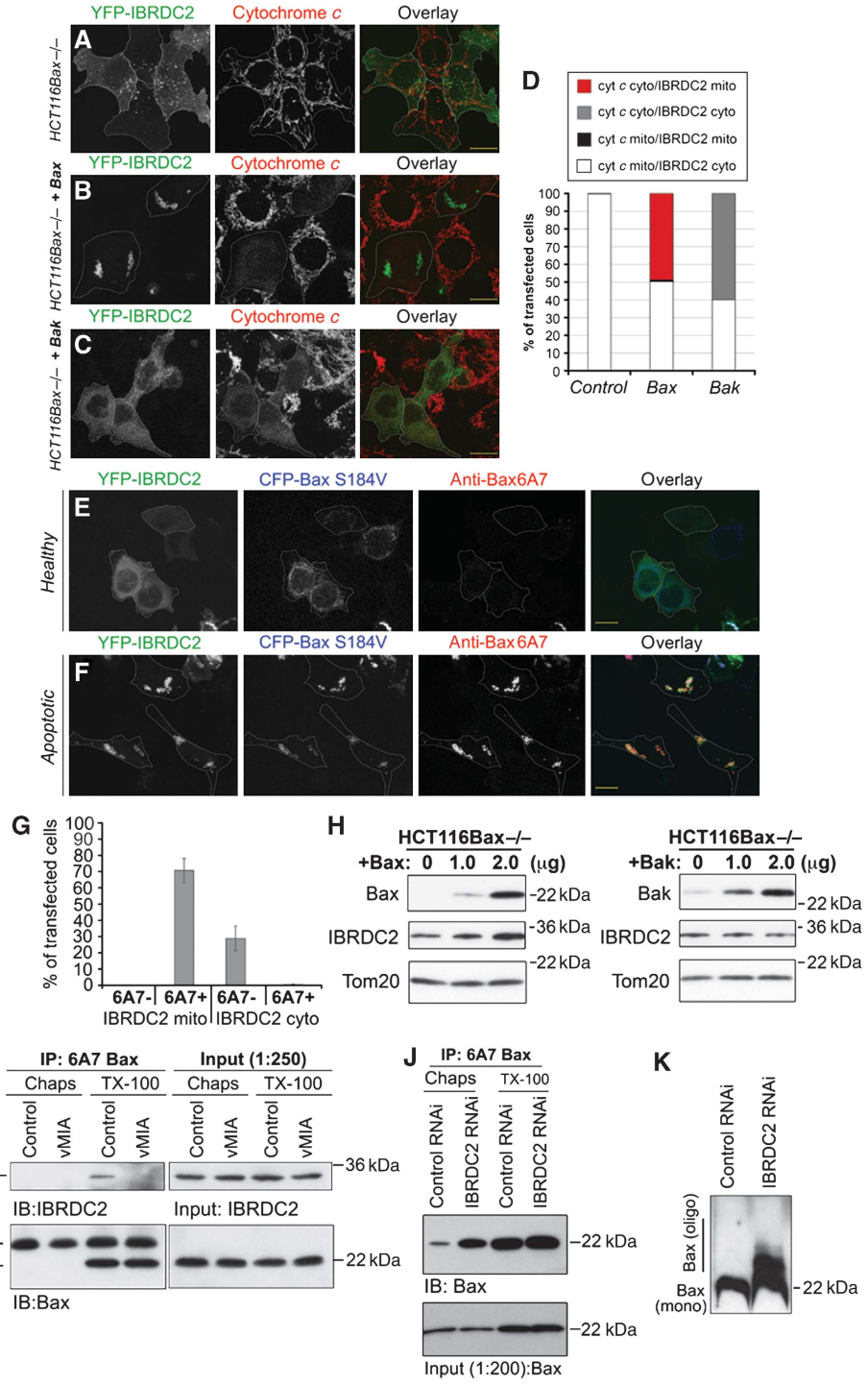

Figure 8 Activated Bax is required and sufficient for mitochondrial accumulation of IBRDC2. HCT116 $Bax^{-/-}$ cells were transfected with YFP-IBRDC2 (green) alone (**A**) or together with Bax (**B**) or Bak (**C**), immunostained for cytochrome *c* (red) and then analysed by confocal microscopy. The apoptosis induction in both Bax- and Bak-overexpressing HCT116 $Bax^{-/-}$ cells was revealed by cytochrome *c* release from the mitochondria to the cytosol (**B**, **C**; middle panels). Bars: 20 μm. (**D**) HCT116 $Bax^{-/-}$ cells transfected as in **A**–**C** were grouped based on the subcellular localizations of cytochrome *c* and IBRDC2 (for details see figure). (**E**, **F**) HCT116$Bax^{-/-}$ cells were transfected with YFP-IBRDC2 together with CFP-Bax^{S184V}. To reveal apoptotic activation of Bax, cells were immunostained with antibodies against the 6A7 epitope of Bax and then analysed by confocal microscopy. Bars: 20 μm. (**G**) Subcellular localization of YFP-IBRDC2 in CFP- Bax^{S184V}-expressing cells 6A7 epitope-negative (as in **E**) and positive (as in **F**) is quantified. Data represent the average ± s.d. of three experiments with >150 cells counted each time. (**H**) Western blot analyses of endogenous IBRDC2 associated with mitochondria in Bax- or Bak-overexpressing HCT116$Bax^{-/-}$ cells. Cells were transfected with indicated amounts of DNA, and then 16 h after transfection were treated with 10 μM ActD for 3 h to induce apoptosis, followed by cell fractionation and western blot analyses of mitochondria-enriched HM fraction, as indicated in the figure. (**I**) Coimmunoprecipitation of 6A7 Bax and IBRDC2 from Chaps and Triton X-100 lysates of control cells and cells expressing vMIA. (**J**) Immunoprecipitation of 6A7 epitope-positive Bax from Chaps and Triton X-100 lysates of IBRDC2 RNAi and Control RNAi cells. (**K**) Control RNAi and IBRDC2 RNAi cells were analysed with BN-PAGE for oligomerization status of Bax.

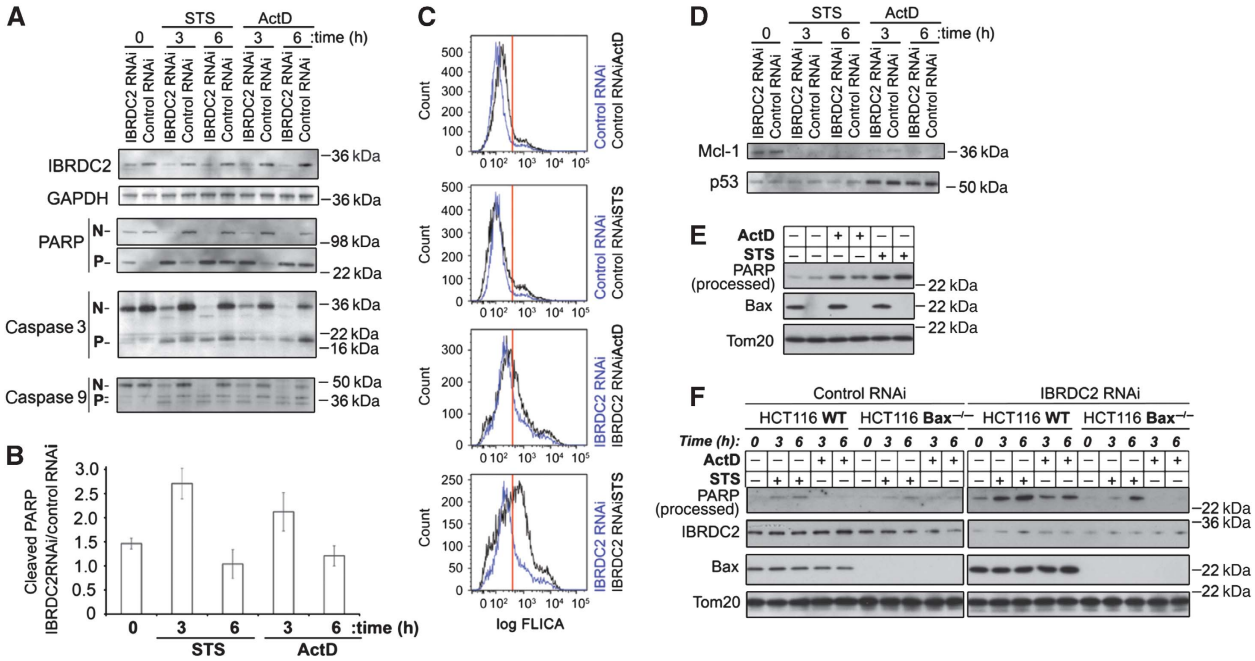

Figure 9 Role of IBRDC2 in the regulation of apoptosis. (**A**) IBRDC2 RNAi and Control RNAi cells were treated with 1 μM STS or 10 μM ActD for 3 h and 6 h and analysed with western blot for PARP cleavage, caspase-3 and caspase-9 activation, IBRDC2 and GAPDH (loading control). 'N' refers to full-length proteins, 'P' processed proteins. (**B**) Quantification of PARP cleavage in IBRDC2 RNAi versus Control RNAi cells. Western blots were scanned and intensities of cleaved PARP bends were quantified using ImageJ software. The data were normalized with cleaved PARP in Control RNAi taken as 1.0 in each analysed sample ($n = 3$). (**C**) Untreated IBRDC2 RNAi (blue lines; two bottom panels) and Control RNAi (blue lines; two top panels), and cells treated with ActD (black lines) and STS (black lines) for 5 h were incubated for 1 h with caspase-3- and caspase-7-specific FLICA reagent and then analysed with FACS. Red line indicates the border between FLICA-negative and FLICA-positive cells. (**D**) IBRDC2 RNAi cells and Control RNAi cells were treated as in **A** and analysed with western blot for changes in protein levels of Mcl-1 and p53. (**E**) Control vector transfected WT and Bax$^{-/-}$ HCT116 cells were treated with 10 μM ActD or 1 μM STS for 10 h, followed by western blot with antibodies indicated in the figure. (**F**) IBRDC2 RNAi WT or Bax$^{-/-}$ HCT116 cells and Control RNAi WT or Bax$^{-/-}$ HCT116 cells were treated with 1 μM STS or 10 μM ActD for 3 h and 6 h and analysed for PARP processing. To confirm the RNAi efficiency in HCT116 cells, the same membranes were also stained with anti-IBRDC2 mAb, anti-Bax mAb and anti-Tom20 polyclonal antibody (loading control).

IBRDC2 RNAi than in Control RNAi cells was also detected at 5 h of treatment with ActD or STS (Figure 9C), indicating a higher sensitivity to ActD- and STS-induced apoptosis in cells with lowered levels of IBRDC2. On the other hand, Mcl-1 degradation and ActD-induced DNA-damage-dependent stabilization of p53, the early ubiquitination-dependent events in apoptosis (Zhong *et al*, 2005; Ringshausen *et al*, 2006), are IBRDC2 protein-level independent (Figure 9D), suggesting that the initial cellular stress response itself is not noticeably affected by IBRDC2 downregulation. Yet, the increased activity of caspases in IBRDC2 RNAi cells (Figure 9A and C) indicates that abnormal apoptosis activation is a response to reduced levels of IBRDC2.

To test the role of Bax in IBRDC2 downregulation-induced apoptosis, we applied IBRDC2 shRNAi in WT and Bax$^{-/-}$ HCT116 cells. As it has been shown that targeted disruption of the *Bax* gene in HCT116 cells renders the cells resistant to apoptosis induced by various unrelated stimuli, we first tested sensitivity of these cells to ActD- and STS-induced apoptosis. To normalize treatment conditions with RNAi cells, HCT116 WT and HCT116 Bax$^{-/-}$cells were first transfected with pEYFP vector, and then 18 h after transfection treated with 10 μM ActD and 1 μM STS for 10 h. We found that treatment with ActD or STS resulted in increased PARP cleavage in Bax$^{-/-}$ HCT116 cells that was only slightly less apparent than in HCT116 WT cells (Figure 9E). Next, Control and IBRDC2 RNAi WT and Bax$^{-/-}$ HCT116 cells were treated with the same concentrations of ActD and STS for 3 h and 6 h and analysed using western blot for PARP cleavage (Figure 9F). The data showed an increase in PARP cleavage in HCT116 WT IBRDC2 RNAi cells that was much less apparent in HCT116 Bax$^{-/-}$ IBRDC2 RNAi cells when compared with respective Control RNAi cells.

In sum, these data indicate that loss of IBRDC2 activity sensitizes cells to Bax-dependent apoptosis. However, as IBRDC2 overexpression does not seem to affect cell survival (Supplementary Figure S6), IBRDC2 is not an anti-apoptotic protein *per se*.

Discussion

In this study we show that IBRDC2, a RING domain E3 Ub ligase, is vital for the control of cell sensitivity to stress-induced apoptosis. The data suggest that IBRDC2 activity is required for protection from the potentially toxic effects of accumulation of activated Bax. This notion is based on several independent lines of evidence: (1) Downregulation of IBRDC2 leads to an abnormal accumulation of activated Bax, as evidenced by highly elevated Bax oligomerization and accumulation of 6A7 epitope-positive Bax in IBRDC2 RNAi cells. (2) Although overexpression of IBRDC2 destabilizes Bax and leads to increases in Bax ubiquitination, downregulation of IBRDC2 increases Bax stability. (3) An apoptosis-specific conformation of Bax is required and sufficient for

mitochondrial accumulation of IBRDC2. (4) IBRDC2 interacts with 6A7 epitope-positive Bax, but not 6A7 epitope-negative Bax. Data showing an increase in IBRDC2-dependent ubiquitination of Bax in apoptotic cells, and thus cells with increased amounts of activated Bax, support this scenario too.

We also found that the mitochondrial translocation-deficient mutant of IBRDC2 does not affect ubiquitination of Bax, suggesting that IBRDC2 indeed targets mitochondria-localized protein. Consistent with this, it has been shown that Bax degradation occurs in mitochondria, but not in the cytosol (Liu *et al*, 2008), suggesting that Bax conformational changes might be recognized by the Ub conjugation machinery and serve as a regulatory mechanism preventing the accumulation of potentially dangerous active Bax in healthy cells. This notion is supported by the fact that mitochondrial localization and the apoptotic conformation of Bax are specifically required for movement of IBRDC2 from the cytosol to the mitochondria. Consistent with this, Bax^{S184V}, a mutant of Bax constitutively associated with mitochondria but showing a non-apoptotic (6A7 epitope-negative) conformation (Nechushtan *et al*, 1999), failed to recruit IBRDC2 to the mitochondria in healthy cells before apoptotic activation. Importantly, because in apoptotic HCT116 $Bax^{-/-}$ cells IBRDC2 does not translocate to the mitochondria, the activated form of Bax, but not Bak or apoptosis-related alterations of mitochondria, seems to be not only required, but also sufficient for mitochondrial accumulation of IBRDC2.

Our findings suggest the existence of an Ub- and IBRDC2-dependent apoptosis checkpoint safeguarding mitochondria from Bax-dependent damage and thus cells from unprompted apoptosis. This mechanism might resemble ubiquitination-dependent regulation of caspases, important for the suppression of unwanted caspase activation (Salvesen and Duckett, 2002; Wilson *et al*, 2002; Morizane *et al*, 2005; Vaux and Silke, 2005; Schile *et al*, 2008). Until the appropriate pro-apoptotic signal level is reached, inhibitor-of-apoptosis proteins (IAPs) suppress the activity of caspases (Wilson *et al*, 2002; Morizane *et al*, 2005; Schile *et al*, 2008). It has been shown that in mammalian cells IAPs might specifically bind processed/activated caspases (Morizane *et al*, 2005), thus preventing the cascade of caspase activation. We propose that IBRDC2 might have similar IAP-like function in the regulation of activated Bax degradation. Yet, in contrast to IAPs and a number of anti-apoptotic proteins from the Bcl-2 family (e.g. Bcl-xL or Mcl-1), overexpression of IBRDC2 does not protect cells from ActD-, STS- or Bax/Bak overexpression-induced apoptosis, even though a massive mitochondrial accumulation of IBRDC2 occurs. One possibility is that IBRDC2 exerts an effect in concert with other proteins, and increasing the levels of IBRDC2 itself without increases in the levels of its putative cofactors is not sufficient to protect cells from apoptosis. However, as we show in this study, ectopic expression of IBRDC2 increases Bax ubiquitination, as well as slightly reduces levels of mitochondria-associated Bax in both healthy and apoptotic cells, indicating that IBRDC2 expression levels influence the rates of Bax ubiquitination and degradation, and thus, supporting the notion that ectopically expressed IBRDC2 is an active protein. Furthermore, overexpression of Bcl-xL, an anti-apoptotic protein known to suppress Bax activation, also inhibits mitochondrial accumulation of IBRDC2. Finally, the data showed that in a subset of untreated cells ($<1\%$), mitochondrial accumulation of IBRDC2 can also be detected, which would not be expected if IBRDC2 was exerting an effect directly as an anti-apoptotic protein. Thus, a more likely alternative is that IBRDC2 does not function as an anti-apoptotic protein *per se*, but is required for Bax control in non-apoptotic cells. In such a scenario, mitochondrial accumulation of IBRDC2 in apoptotic cells would follow a massive mitochondrial accumulation of the IBRDC2 substrate, 6A7 epitope-positive Bax, but not represent any regulatory anti- or pro-apoptotic activity for IBRDC2.

The data shown in this study support a model in which IBRDC2-dependent elimination of the 6A7-positive form of Bax is critical in non-apoptotic cells for protection against mitochondrial toxicity of activated Bax, without an effect on Bax activation itself. In such a scenario IBRDC2 would exert an effect downstream of anti-apoptotic proteins from the Bcl-2 family and other factors implicated in the regulation of Bax activation. Consistent with this, ectopic expression of Bcl-xL inhibits mitochondrial accumulation of IBRDC2 and likely regulates physical interaction of IBRDC2 and Bax. However, untreated cells with reduced levels of endogenous IBRDC2 show an abnormal accumulation of active Bax, and perhaps as a consequence of this, are spontaneously dying through apoptosis without any external pro-apoptotic stimuli. Furthermore, as HCT116 $Bax^{-/-}$ cells are not sensitized to apoptosis by IBRDC2 downregulation, it is likely that loss of IBRDC2 activity is specifically linked to Bax, but not other changes in cell physiology. The physical interaction of IBRDC2 and 6A7 epitope-positive Bax in untreated cells further support the specific role of IBRDC2 in the regulation of Bax fate. Bearing in mind that overexpression of Bax or Bak induces or sensitizes cells to apoptosis (Nechushtan *et al*, 1999; Schinzel *et al*, 2004) and that these proteins can be activated in a cascade in which activated proteins induce activation of latent proteins (Ruffolo and Shore, 2003; Tan *et al*, 2006; Liu *et al*, 2008), early elimination of activated Bax is likely to be critical for cell survival. Indeed, supporting the possibility that self-activation of Bcl-2 family proteins has a significant role in apoptosis activation, it has been shown that an activated Bak mutant induced a conformation change in, and oligomerization of, non-activated Bak (Ruffolo and Shore, 2003). This notion has been further corroborated by the data showing that truncated Bax (H2-H3) could activate full-length Bax (Tan *et al*, 2006). Thus, as H2-H3 mimics the part of Bax that, under physiological conditions, is exposed after Bax is activated by BH3-only proteins, it has been proposed that active Bax-induced Bax activation occurs during apoptosis (Tan *et al*, 2006). Therefore, to prevent a self-accelerating Bax activation cascade, active Bax needs to be both neutralized through the activity of anti-apoptotic Bcl-2 family proteins and as we suggest, removed/degraded through the IBRDC2- and Ub-dependent pathway. One could speculate that the removal of active Bax may be particularly relevant when a subthreshold BH3-only protein-dependent apoptotic signal is overcome by a strong anti-apoptotic response. On the other hand, as overexpression of IBRDC2 does not affect apoptosis triggered by ActD, STS or Bax overexpression, which are strong apoptosis inducers able to overcome anti-apoptotic Bcl-2 family proteins, elimination of activated Bax in cells destined to die is not sufficient to affect the rates of apoptosis. This notion is supported by the very low anti-apoptotic effect of IBRDC2 ectopic expression.

Materials and methods

Cell culture and transfection

HeLa cells were cultured in DMEM medium supplemented with 10% heat-inactivated fetal bovine serum, 2 mM Glutamax, 1 mM sodium pyruvate, MEM non-essential amino acids (GIBCO), 100 U/ml penicillin and 100 μg/ml streptomycin in 5% CO_2 at 37°C. HCT116 cells were cultured in McCoy's 5A medium supplemented with 10% heat-inactivated fetal bovine serum, 2 mM Glutamax, 1 mM sodium pyruvate and 100 U/ml penicillin and 100 μg/ml streptomycin in 5% CO_2 at 37°C. HCT 116 Bak$^{-/-}$ cells were obtained by deletion of the *Bak* gene by homologous recombination in the HCT116 WT cells (Wang and Youle, manuscript in preparation). Cells were transfected with FuGene 6 (Roche; for microscopy) or with FuGeneHD (Roche; for protein lysates) according to the manufacturer's instructions.

Cloning

PCR fragments of IBRDC2 were generated using the proofreading *Pfx* DNA polymerase (Invitrogen) from commercially available cDNA clone (IMAGE_30331343; Invitrogen) as template. The primers used were: 5′-CTAGACTAAGCTTCCATGGGCTCAGCTGG TAGGC-3′ and 3′-ACTAGGGATCCCCGGTTGTGGATGGGTCGTGCTT-5′. PCR fragments were purified, digested with the appropriate restriction enzymes and cloned into respective YFP (pEYFP-C1, Clontech) and 3MYC-tag (pCMV-3Tag-2, Stratagene) encoding vectors to generate YFP-IBRDC2 or 3MYC-IBRDC2. Inactive RING mutant was generated by site-directed mutagenesis of the respective plasmids using *Pfu* Turbo DNA polymerase (Stratagene) with the primers: 5′-GTTGCAAGGATGCTTGGTGGGCAGAGGTATCCTGTAGA GACAGTCAG-3′ and 5′-CTGACTGTCTCTACAGGATACCTCTGCCCAC CAAGCATCCTTGCAAC-3′ changing the crucial histidine codons in the RING domain to tryptophan codons. For the generation of YFP-IBRDC2Δ^{TM}, IBRDC2 was amplified using 5′-CTAGACTAAGCTTCCA TGGGCTCAGCTGGTAGGC-3′ and 5′-CTAGAAGCTTCCTTAGCCCCG ACAGGACTTGCAGAC-3′ and cloned into YFP-C1. All constructs were verified by sequencing. pCDNA3.1-BAX, CFP-Bax, YFP-Bax, CFP-Bax^{S184V} and CFP-Bak were described previously (Nechushtan *et al*, 1999, 2001; Karbowski *et al*, 2002). The short hairpin RNAi was performed using commercially available IBRDC2 shRNAi constructs (Thermo Scientific and Sigma). shRNAi constructs targeted were: 1: 893-CGGGTTTATATCGAACGCAAT-913; 2: 569-GCTGAGATTGCCTGTTTGGTA-589 and 3: 593-GTGGACCAGTTTCA ACTTTAT-613, sequences of the reference human IBRDC2 mRNA (Gene bank no. NM_182757.2) GFP shRNAi construct (Thermo Scientific) was used as control. Cells were transfected with respective constructs, and then ∼24 h after transfection, to select transfected cells, they were incubated with 3 μg/ml puromycine for additional 3 days.

Western blot and immunoprecipitation

Cells were harvested and total cell protein lysates and cell fractionations were prepared as previously described (Karbowski *et al*, 2007). Protein lysates were analysed by western blot using: anti-Bax mAb (BD Biosciences), anti-IBRDC2 mAb (Abcam or Sigma), anti-Tom20 polyclonal antibody (Santa Cruz), anti-Ub polyclonal antibody (Santa Cruz), anti-Drp1 mAb (BD Biosciences), anti-Complex I (subunit 21-kD; Mitosciences), anti-GAPDH polyclonal antibody (Abcam), anti-PARP polyclonal antibody (Imgenex), anti-caspase 3 mAb (Imgenex), anti-caspase 9 mAb (Imgenex), anti-p53 mAb (Imgenex) anti-Mcl-1 mAb (BD Biosciences), anti-Bcl-xL mAb (BD Biosciences), anti-Bcl-2 mAb (BD Biosciences), anti-Bak mAb (BD Biosciences) and anti-Myc tag mAb (Roche). Immunoprecipitation was performed as described (Norris and Youle, 2008). Blue Native PAGE was performed with NativePAGE Bis-Tris gel system, using cell lysates obtained with 1% DDM, following the manufacture's recommendations (Invitrogen).

Immunofluorescence and confocal microscopy

The immunofluorescence and confocal microscopy analyses were performed as previously described (Karbowski *et al*, 2007). The primary antibodies used for immunofluorescence studies were: anti-Tom20 polyclonal antibody (Santa Cruz), anti-cytochrome *c* mAb (BD Biosciences) and anti-Bax 6A7 mAb (Abcam). Images were acquired with a Zeiss LSM510 confocal microscope (Zeiss Microlimaging), using a × 100/1.45 α-Plan-FLUAR objective lens or ApoTome- and AxioCamMRm Rev.3 camera-equipped AxioObserver Z1 (Zeiss Microlmaging), using × 100/1.4 Plan-Apochromat objective lens. Projections of 12-bit confocal z-sections (interval 0.25 μm) covering the entire depth of the cell, or single z-sections obtained with AxioObserver Z1 were used. Live cell confocal microscopy experiments were performed as previously described (Karbowski *et al*, 2002, 2007). Colocalization analyses were performed using colocalization module of AxioVision 4 software.

FACS analyses

Activity of caspase-3 and -7 was analysed using Vybrant FAM Caspase-3 and -7 Assay Kit (Invitrogen) following the manufacture's instructions.

Supplementary data

Supplementary data are available at *The EMBO Journal* Online (http://www.embojournal.org).

Acknowledgements

We thank Pamela Wright for comments on the paper, Xu Shan for technical support, and James W Nagle and Debbie Kaufmann from the NINDS DNA sequencing facility for the excellent service provided. We also gratefully acknowledge financial support from the National Institute of General Medical Science RO1 GM083131 (MK).

Conflict of interest

The authors declare that they have no conflict of interest.

References

Adams JM, Cory S (2007) The Bcl-2 apoptotic switch in cancer development and therapy. *Oncogene* **26:** 1324–1337

Agrawal SG, Liu FT, Wiseman C, Shirali S, Liu H, Lillington D, Du MQ, Syndercombe-Court D, Newland AC, Gribben JG, Jia L (2008) Increased proteasomal degradation of Bax is a common feature of poor prognosis chronic lymphocytic leukemia. *Blood* **111:** 2790–2796

Aleo E, Henderson CJ, Fontanini A, Solazzo B, Brancolini C (2006) Identification of new compounds that trigger apoptosome-independent caspase activation and apoptosis. *Cancer Res* **66:** 9235–9244

Arnoult D, Bartle LM, Skaletskaya A, Poncet D, Zamzami N, Park PU, Sharpe J, Youle RJ, Goldmacher VS (2004) Cytomegalovirus cell death suppressor vMIA blocks Bax- but not Bak-mediated apoptosis by binding and sequestering Bax at mitochondria. *Proc Natl Acad Sci USA* **101:** 7988–7993

Azad N, Vallyathan V, Wang L, Tantishaiyakul V, Stehlik C, Leonard SS, Rojanasakul Y (2006) S-nitrosylation of Bcl-2 inhibits its ubiquitin-proteasomal degradation. A novel antiapoptotic mechanism that suppresses apoptosis. *J Biol Chem* **281:** 34124–34134

Braschi E, Zunino R, McBride HM (2009) MAPL is a new mitochondrial SUMO E3 ligase that regulates mitochondrial fission. *EMBO Rep* **10:** 748–754

Breitschopf K, Haendeler J, Malchow P, Zeiher AM, Dimmeler S (2000) Posttranslational modification of Bcl-2 facilitates its proteasome-dependent degradation: molecular characterization of the involved signaling pathway. *Mol Cell Biol* **20:** 1886–1896

Chipuk JE, Green DR (2008) How do BCL-2 proteins induce mitochondrial outer membrane permeabilization? *Trends Cell Biol* **18:** 157–164

Cuconati A, Mukherjee C, Perez D, White E (2003) DNA damage response and MCL-1 destruction initiate apoptosis in adenovirus-infected cells. *Genes Dev* **17:** 2922–2932

Datta SR, Ranger AM, Lin MZ, Sturgill JF, Ma YC, Cowan CW, Dikkes P, Korsmeyer SJ, Greenberg ME (2002) Survival factor-mediated BAD phosphorylation raises the mitochondrial threshold for apoptosis. *Dev Cell* **3:** 631–643

De Giorgi F, Lartigue L, Bauer MK, Schubert A, Grimm S, Hanson GT, Remington SJ, Youle RJ, Ichas F (2002) The permeability transition pore signals apoptosis by directing Bax translocation and multimerization. *FASEB J* **16:** 607–609

Fang S, Lorick KL, Jensen JP, Weissman AM (2003) RING finger ubiquitin protein ligases: implications for tumorigenesis, metastasis and for molecular targets in cancer. *Semin Cancer Biol* **13:** 5–14

Fontanini A, Foti C, Potu H, Crivellato E, Maestro R, Bernardi P, Demarchi F, Brancolini C (2009) The isopeptidase inhibitor G5 triggers a caspase-independent necrotic death in cells resistant to apoptosis: a comparative study with the proteasome inhibitor bortezomib. *J Biol Chem* **284:** 8369–8381

Fu NY, Sukumaran SK, Kerk SY, Yu VC (2009) Baxbeta: a constitutively active human Bax isoform that is under tight regulatory control by the proteasomal degradation mechanism. *Mol Cell* **33:** 15–29

Hershko A, Ciechanover A (1992) The ubiquitin system for protein degradation. *Annu Rev Biochem* **61:** 761–807

Hershko A, Ciechanover A (1998) The ubiquitin system. *Annu Rev Biochem* **67:** 425–479

Hsu YT, Wolter KG, Youle RJ (1997) Cytosol-to-membrane redistribution of Bax and Bcl-X(L) during apoptosis. *Proc Natl Acad Sci USA* **94:** 3668–3672

Hsu YT, Youle RJ (1998) Bax in murine thymus is a soluble monomeric protein that displays differential detergent-induced conformations. *J Biol Chem* **273:** 10777–10783

Huang J, Xu LG, Liu T, Zhai Z, Shu HB (2006) The p53-inducible E3 ubiquitin ligase p53RFP induces p53-dependent apoptosis. *FEBS Lett* **580:** 940–947

Joazeiro CA, Weissman AM (2000) RING finger proteins: mediators of ubiquitin ligase activity. *Cell* **102:** 549–552

Karbowski M, Lee YJ, Gaume B, Jeong SY, Frank S, Nechushtan A, Santel A, Fuller M, Smith CL, Youle RJ (2002) Spatial and temporal association of Bax with mitochondrial fission sites, Drp1, and Mfn2 during apoptosis. *J Cell Biol* **159:** 931–938

Karbowski M, Neutzner A, Youle RJ (2007) The mitochondrial E3 ubiquitin ligase MARCH5 is required for Drp1 dependent mitochondrial division. *J Cell Biol* **178:** 71–84

Kluck RM, Bossy-Wetzel E, Green DR, Newmeyer DD (1997) The release of cytochrome *c* from mitochondria: a primary site for Bcl-2 regulation of apoptosis. *Science* **275:** 1132–1136

Li W, Bengtson M, Ulbrich A, Matsuda A, Reddy V, Orth A, Chanda S, Batalov S, Joazeiro C (2008) Genome-wide and functional annotation of human E3 ubiquitin ligases identifies MULAN, a mitochondrial E3 that regulates the organelle's dynamics and signaling. *PLoS ONE* **23:** e1487

Liu FT, Agrawal SG, Gribben JG, Ye H, Du MQ, Newland AC, Jia L (2008) Bortezomib blocks Bax degradation in malignant B cells during treatment with TRAIL. *Blood* **111:** 2797–2805

Marin I, Lucas JI, Gradilla AC, Ferrus A (2004) Parkin and relatives: the RBR family of ubiquitin ligases. *Physiol Genomics* **17:** 253–263,

Morizane Y, Honda R, Fukami K, Yasuda H (2005) X-linked inhibitor of apoptosis functions as ubiquitin ligase toward mature caspase-9 and cytosolic Smac/DIABLO. *J Biochem* **137:** 125–132

Nakamura N, Kimura Y, Tokuda M, Honda S, Hirose S (2006) MARCH-V is a novel mitofusin 2- and Drp1-binding protein able to change mitochondrial morphology. *EMBO Rep* **7:** 1019–1022

Nakano K, Vousden KH (2001) PUMA, a novel proapoptotic gene, is induced by p53. *Mol Cell* **7:** 683–694

Narendra D, Tanaka A, Suen DF, Youle RJ (2008) Parkin is recruited selectively to impaired mitochondria and promotes their autophagy. *J Cell Biol* **183:** 795–803

Nechushtan A, Smith CL, Hsu YT, Youle RJ (1999) Conformation of the Bax C-terminus regulates subcellular location and cell death. *EMBOJ* **18:** 2330–2341

Nechushtan A, Smith CL, Lamensdorf I, Yoon SH, Youle RJ (2001) Bax and Bak coalesce into novel mitochondria-associated clusters during apoptosis. *J Cell Biol* **153:** 1265–1276

Ng CC, Arakawa H, Fukuda S, Kondoh H, Nakamura Y (2003) p53RFP, a p53-inducible RING-finger protein, regulates the stability of p21WAF1. *Oncogene* **22:** 4449–4458

Norris KL, Youle RJ (2008) Cytomegalovirus proteins vMIA and m38.5 link mitochondrial morphogenesis to Bcl-2 family proteins. *J Virol* **82:** 6232–6243

Ringshausen I, O'Shea CC, Finch AJ, Swigart LB, Evan GI (2006) Mdm2 is critically and continuously required to suppress lethal p53 activity *in vivo*. *Cancer Cell* **10:** 501–514

Ruffolo SC, Shore GC (2003) BCL-2 selectively interacts with the BID-induced open conformer of BAK, inhibiting BAK auto-oligomerization. *J Biol Chem* **278:** 25039–25045

Salvesen GS, Duckett CS (2002) IAP proteins: blocking the road to death's door. *Nat Rev Mol Cell Biol* **3:** 401–410

Schile AJ, Garcia-Fernandez M, Steller H (2008) Regulation of apoptosis by XIAP ubiquitin-ligase activity. *Genes Dev* **22:** 2256–2266

Schinzel A, Kaufmann T, Schuler M, Martinalbo J, Grubb D, Borner C (2004) Conformational control of Bax localization and apoptotic activity by Pro168. *J Cell Biol* **164:** 1021–1032

Tait SW, de Vries E, Maas C, Keller AM, D'Santos CS, Borst J (2007) Apoptosis induction by Bid requires unconventional ubiquitination and degradation of its N-terminal fragment. *J Cell Biol* **179:** 1453–1466

Tan C, Dlugosz PJ, Peng J, Zhang Z, Lapolla SM, Plafker SM, Andrews DW, Lin J (2006) Auto-activation of the apoptosis protein Bax increases mitochondrial membrane permeability and is inhibited by Bcl-2. *J Biol Chem* **281:** 14764–14775

Vaux DL, Silke J (2005) IAPs, RINGs and ubiquitylation. *Nat Rev Mol Cell Biol* **6:** 287–297

Villunger A, Michalak EM, Coultas L, Mullauer F, Bock G, Ausserlechner MJ, Adams JM, Strasser A (2003) p53- and drug-induced apoptotic responses mediated by BH3-only proteins puma and noxa. *Science* **302:** 1036–1038

Wei MC, Zong WX, Cheng EH, Lindsten T, Panoutsakopoulou V, Ross AJ, Roth KA, MacGregor GR, Thompson CB, Korsmeyer SJ (2001) Proapoptotic BAX and BAK: a requisite gateway to mitochondrial dysfunction and death. *Science* **292:** 727–730

Wilson R, Goyal L, Ditzel M, Zachariou A, Baker DA, Agapite J, Steller H, Meier P (2002) The DIAP1 RING finger mediates ubiquitination of Dronc and is indispensable for regulating apoptosis. *Nat Cell Biol* **4:** 445–450

Yonashiro R, Ishido S, Kyo S, Fukuda T, Goto E, Matsuki Y, Ohmura-Hoshino M, Sada K, Hotta H, Yamamura H, Inatome R, Yanagi S (2006) A novel mitochondrial ubiquitin ligase plays a critical role in mitochondrial dynamics. *EMBOJ* **25:** 3618–3626

Youle RJ, Strasser A (2008) The BCL-2 protein family: opposing activities that mediate cell death. *Nat Rev Mol Cell Biol* **9:** 47–59

Zhang B, Huang J, Li H, Liu T, Wang Y, Waterman P, Mao A, Xu L, Zhai Z, Liu D, Marrack P, Sju H (2008) GIDE is a mitochondrial E3 ubiquitin ligase that induces apoptosis and slows growth. *Cell Res* **18:** 900–910

Zhong Q, Gao W, Du F, Wang X (2005) Mule/ARF-BP1, a BH3-only E3 ubiquitin ligase, catalyzes the polyubiquitination of Mcl-1 and regulates apoptosis. *Cell* **121:** 1085–1095

Zunino R, Schauss A, Rippstein P, Andrade-Navarro M, McBride HM (2007) The SUMO protease SENP5 is required to maintain mitochondrial morphology and function. *J Cell Sci* **120:** 1178–1188